Additive-free superhard B_4C with ultrafine-grained dense microstructures

B. Malmal Moshtaghioun [a,*], Francisco L. Cumbrera [a], Angel L. Ortiz [b], Miguel Castillo-Rodríguez [c], Diego Gómez-García [a,c]

[a] *Departamento de Física de la Materia Condensada, Universidad de Sevilla, 41012 Sevilla, Spain*
[b] *Departamento de Ingeniería Mecánica, Energética y de los Materiales, Universidad de Extremadura, 06006 Badajoz, Spain*
[c] *Instituto de Ciencia de Materiales, CSIC-Universidad de Sevilla, 41092 Sevilla, Spain*

Abstract

A unique combination of high-energy ball-milling, annealing, and spark-plasma sintering has been used to process superhard B4 C ceramics with ultrafine-grained, dense microstructures from commercially available powders, without sintering additives. It was found that the ultrafine powder prepared by high-energy ball-milling is hardly at all sinterable, but that B2 O3 removal by gentle annealing in Ar provides the desired sinterability. A parametric study was also conducted to elucidate the role of the temperature (1600–1800 ◦ C), time (1–9 min), and heating ramp (100 or 200 ◦ C/min) in the densification and grain growth, and thus to identify optimal spark-plasma sintering conditions (i.e., 1700 ◦ C for 3 min with 100 ◦ C/min) to densify completely (>98.5%) the B4 C ceramics with retention of ultrafine grains (∼370 nm). Super-high hardness of ∼38 GPa without relevant loss of toughness (∼3 MPa m1/2) was thus achieved, attributable to the smaller grain size and to the transgranular fracture mode of the B4 C ceramics.

1. Introduction

There is great interest in the processing of superhard poly- crystalline ceramics with refined microstructures for their use in a wide variety of structural applications, including wear parts, cutting tools, bearings, mechanical seals, valves, rollers, noz- zles, rotors, filters, to cite just some. Boron carbide (B4 C) is one of the short list of the family of superhard ceramics, and has captured the growing attention of the ceramics community because its super-high hardness is accompanied by a low density (∼2.52 g cm−3), high melting point (∼2540 ◦C), good chemical inertness, high Young's modulus (∼445 GPa), and high thermal conductivity (∼30 W m−1 K−1), among other physicochemical properties.1–3 With this attractive set of properties, B4 C is a leading candidate material for many advanced contact-mechanical and tribological applications. For example, it is being extensively investigated as a lightweight armour material. It also has a large

neutron absorption cross-section, and is used as shielding and control rods in some current fission reactors, and is being actively investigated for the next generation of fast reactors.4 Furthermore, like SiC, B4 C is a high-temperature semiconductor that could potentially be used for novel electronic applications.3 While not the primary concern in these latter two applications, the mechanical properties of B4 C are nevertheless always fun- damental to ensure structural integrity under service conditions.

In broad terms, a key problem that has plagued research on B4 C ceramics is its fabrication. Traditionally, B4 C polycrystalline ceramics have been fabricated either by con- ventional pressureless sintering or hot-pressing at very high temperatures,2,5 which nonetheless have the drawback that the resulting ceramics normally possess a porous microstructure of coarse grain size (to a greater or lesser extent depending on the exact sintering conditions) that makes them not especially super-hard. Sintering additives have been used to facilitate the densification of B4 C ceramics,2 but they lead to greater grain growth and the consequent loss of theoretical hardness. B4 C has also been fabricated by hot-isostatic pressing (HIP) at very high pressures with encapsulation,2 or by pressureless sintering followed by HIP without encapsulation, but these routes are especially tedious and have obvious drawbacks. Microwave sintering can effectively densify additive-free B4 C at high tem- peratures, but it does not resolve the problem of grain growth.2

More recently, it has been demonstrated that spark-plasma sintering (SPS) has the potential to densify B4 C ceramics and composites without additives,6–12 and, importantly, with only moderate grain growth if the SPS conditions are tuned conveniently.11 This suggests that the goal of processing additive-free superhard B4 C with ultrafine-grained, dense microstructures is in principle potentially attainable if one could start from appropriate ultrafine powders or nanopowders, as can be prepared for example from typical commercially available submicrometric powders by high-energy ball-milling. This was thus the objective of the present work, which was conducted to demonstrate the feasibility of this processing approach by a parametric study (in particular, temperature, time, and heating ramp) of the densification and grain growth by SPS of a B4 C powder subjected to high-energy ball-milling, together with the subsequent microstructural and mechanical characterizations of the resulting ceramics.

2. Experimental procedure

A commercially available submicrometric powder of B4 C (~0.5 J..m; Grade HD20, H.C. Starck, Germany) was chosen as starting material to prepare an ultrafine B4 C powder. To this end, the as-received powder was subjected to high-energy ball-milling in a shaker mill (Spex D8000, Spex CertiPrep, USA) operated at about 1060 back-and-forth cycles per minute. The high-energy ball-milling was carried out under ambient condi- tions for 180 min in cylindrical hardened-steel containers with WC balls (6.7 mm in diameter; Union Process Inc., USA) at a

ball-to-powder volume ratio of ∼8:1. More details of the milling protocol, including the approach used to minimize the powder contamination by the milling media (i.e., WC) and to avoid the contamination by the container (i.e., Fe),13 have been given elsewhere.12 Preliminary SPS experiments revealed that the ball-milled B4 C powder has poor sinterability despite the high-energy ball- milling having refined the crystal sizes notably. Indeed, it was even more difficult to densify than the as-received submicro-metric powder.11,12 An example of this poor sinterability is shown in Fig. 1. This was attributed to the formation during milling of extra B2 O3 on the surface of the B4 C nanocrystals, which is known to favour coarsening over densification.14,15 Consequently, to enhance its sinterability, the ball-milled B4 C powder was annealed at 1350 ◦C (heating and cooling ramps of 5 ◦C/min) for 8 h in a tubular furnace (TermoLAb TH1700, Portugal) under a flowing atmosphere of ultrahigh purity Ar, which is a heat-treatment that has already proven to be effec- tive for the elimination of the B2 O3 impurities in other boride ceramics16 ; the basis is that B2 O3 melts at ∼510 ◦C and experiences significant evaporation beyond 1000 ◦C, so that even in the absence of chemical reactions the B2 O3 surface impurities can be removed through the phase-change reaction B2 O3 (l) → B2 O3 (g). The resulting powder was then character- ized by scanning electron microscopy (SEM; S5200, Hitachi, Japan), X-ray diffractometry (XRD; D8 Discover, Bruker,

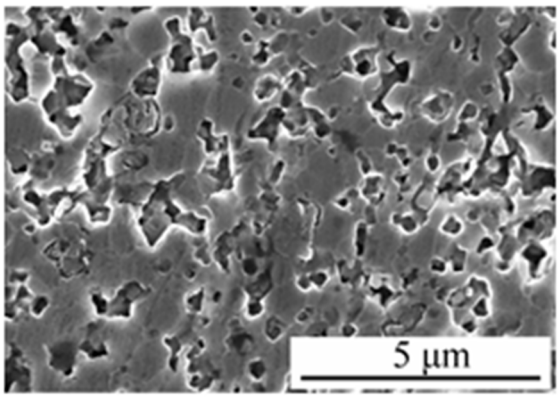

Fig. 1. Representative SEM micrograph of the polished surface of the ceramic resulting from the SPS at 1700 ◦ C for 3 min with heating ramp of 100 ◦ C/min of the B4 C powder subjected to 180 min of high-energy ball-milling.

Germany), and X-ray photoemission spectroscopy (XPS K- Alpha, Thermo Scientific, UK). The SEM observations were done at an accelerating voltage of 5 kV with secondary electrons without additional specimen preparation, and the SEM images were analyzed using image analysis software, the purpose being to measure the particle sizes directly. The XRD pattern was collected in the step-scanning mode (2ϑ range 10–70◦, step width 0.015◦, counting time 5 s) using Cu-Kcx radiation, and was indexed with the aid of the

PDF2 database and analyzed quantita- tively by the Rietveld method (FullProf, version 3.5d)17 with the Thompson-Cox-Hastings profile model and an Al2 O3 sample as standard for the instrumental broadening, the purpose now being to determine the crystalline phases and their relative abundance, and the reasonable estimate of the B4 C crystal sizes. The XPS spectrum of the B 1s core line was recorded in ultra-high vacuum (10−6 Pa) in the 180–196 eV range at 0.1 eV energy resolution using a monochromatic Al-Kcx X-ray source (1486.6 eV), and was indexed using common databases, the purpose here being to identify the bonding environments or statuses.

Next, the ball-milled and annealed B4 C powder was loaded into 15-mm diameter graphite dies lined with graphite foil and surrounded by a 1 cm thick graphite blanket to minimize heat loss, and then spark-plasma sintered (Dr. Sinter 515S, Sumitomo Coal Mining Co., Japan) in a dynamic vacuum (i.e., ~6 Pa) at peak temperatures in the range 1600–1800 ◦C (as measured by an optical pyrometer focused on the die), with soaking times in the interval 1–9 min, heating ramps of 100 or 200 ◦C/min, and uniaxial pressure of 75 MPa (applied during the first minute of heating). Table 1 lists the specific SPS variables used, with the DC pulse sequence always being 12(on):2(off) with pulses of 3.3 ms. This parametric study was performed to identify appro- priate SPS conditions to obtain ultrafine-grained, dense, B4 C microstructures with super-high hardness. More details of the SPS protocol have been given elsewhere.11,12 The relative density of the resulting B4 C ceramics was mea- sured by the Archimedes method using distilled water as the immersion media. The sintered ceramics were also characterized by XRD, SEM coupled with X-ray energy dispersive spec- trometry (XEDS), and transmission electron microscopy (TEM; Philips CM-200) also with XEDS. XRD was used with the same objectives in mind and experimental procedures as in the case of the powder. This latter also applied to the SEM/XEDS analyses, except for the fact that the observations were done on both fracture surfaces and polished surfaces (1-J..m finish using routine ceramographic methods) that had previously been electro-chemically etched with a solution of 1% KOH. Finally, the TEM/XEDS observations were made at an accelerating volt- age of 200 kV, with the specimens prepared using conventional methods applicable to ceramic materials (i.e., successive steps of mechanical thinning, dimpling, and ion-beam milling to per- foration). These electron microscopy procedures were aimed at characterizing the microstructures (i.e., residual porosity, grain sizes, and phase distribution).

Table 1
Processing conditions, microstructural features, and room-temperature mechanical properties of the additive-free B_4C ceramics prepared in this study.

Sample	Sintering conditions[a]			Relative density (%)[b]	Average B_4C grain size (nm)	Mechanical properties	
	Temperature (°C)	Time (min)	Heating ramp (°C/min)			Hardness (GPa)	Toughness ($MPa\,m^{1/2}$)
S1	1800	3	100	99.2	17,200	n.t.	n.t.
S2	1700	9	100	98.7	460	n.t.	n.t.
S3	1700	3	100	98.7	370	37.8	3.1
S4	1700	3	200	98.8	450	37.0	2.9
S5	1700	1	100	97.1	340	36.5	3.1
S6	1700	1	200	97.4	385	37.4	3.0
S7	1650	3	100	96.3	320	34.9	3.6
S8	1650	3	200	97.0	360	36.4	3.4
S9	1650	1	200	95.4	320	n.t.	n.t.
S10	1600	3	100	93.6	300	n.t.	n.t.
S11	1600	3	200	95.1	320	n.t.	n.t.

n.t. means not tested.
[a] Uniaxial pressure of 75 MPa.
[b] Theoretical densities calculated from the quantitative phase-composition determined experimentally.

Polished cross-sections of selected B4 C ceramics were cut along the diameter of the sintered discs, and indented at several different locations (10 indentations per specimen) under a load of 9.81 N using a hardness tester (Struers A/S, DK-2750 Bullerup, Denmark) equipped with a Vickers diamond pyramid. As has already been done before in B4 C ceramics and composites,11,12 the hardness and the toughness were subsequently determined using the standard protocol and expressions18,19 from well- defined Vickers residual imprints exhibiting only radial cracks under optical microscopy.

3. Results and discussion

Fig. 2 shows a representative SEM image of the B4 C powder after the high-energy ball-milling and the subsequent annealing. It can be seen that the powder mostly comprises primary B4 C particles with an average size of ~220 nm and equiaxed shape. There are also a few other larger platelet particles with the morphology of a triangular prism, which is indeed the equilibrium shape of WC. The Rietveld refinement of the corresponding XRD pattern shown in Fig. 3 confirmed that this powder is essentially formed by B4 C (97.3 ± 0.9 wt.%) with small amounts of WC (0.30 ± 0.02 wt.%), C (0.45 ± 0.07 wt.%), W2 B5 (0.79 ± 0.01 wt.%), and WB2 (2.20 ± 0.02 wt.%); some weak XRD peaks could not be indexed, which most likely indicates the additional presence of

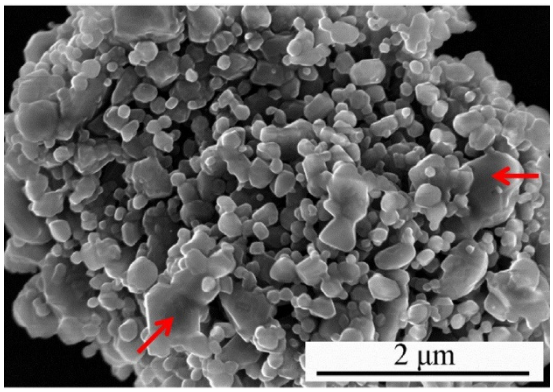

Fig. 2. Representative SEM image of the ultrafine B4 C powder obtained by high-energy ball-milling followed by annealing. The arrows point to particles with the morphology of a triangular prism.

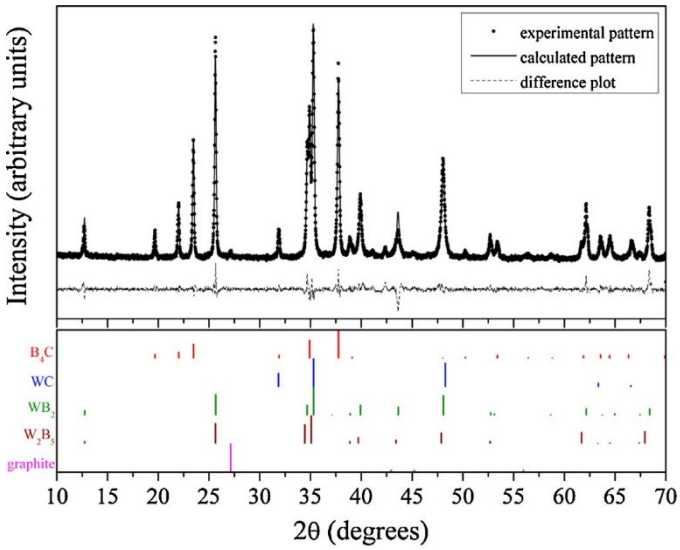

Fig. 3. XRD pattern of the ultrafine B4 C powder obtained by high-energy ball- milling followed by annealing (data point), together with the corresponding Rietveld refinement (solid line). The peak indexing is also included (pdf cards 00-035-0798, 00-051-0939, 01-073-1244, 00-038-1365, and 00-056-0159 for B4 C, WC, WB2 , W2 B5 , and graphite, respectively).

trace amounts of unidentified W-rich phase(s). Unlike WC, graphite and these two latter boride phases are not direct products from the contamination by the milling media, and indeed were not detected in the B4 C powder ball- milled but not annealed, whose quantitative-phase composition was 97.41 ± 0.08 wt.% B4 C plus 2.59 ± 0.05 wt.% WC accord- ing to the corresponding Rietveld refinement of its XRD pattern (not shown). Consequently, the detection of C, W2 B5 , and WB2 reflects the occurrence of reactions between B4 C and WC during the annealing treatment of the ball-milled powder at 1350 ◦C for 8 h in Ar. This might have happened via the set of reactions:

5B4 C + 8WC → 4W2 B5 + 13C

4W2 B5 + C → 8WB2 + B4

(or, W2 B5 → WB2 + B plus 4B + C → B4 C)

and perhaps also via

B4 C + 2WC → 2WB2 + 3C,

with both reaction paths leading to excess of C. This is consistent with the detection of graphite in the XRD pattern of Fig. 3, although it should be mentioned that part of the

graphite generated could also have contributed to eliminat- ing B2 O3 impurities via the carbothermal-reduction reaction B2 O3 + 7C → B4 C + 6CO(g). It is also interesting to note that the analysis of the peak broadening indicated that the B4 C crystallites have an average size of ∼200 nm, which is very similar to the particle size measured by SEM; while the average crystallite size determined from the present Rietveld analyses cannot be regarded as being totally accurate numerically due to the inherent limitations of the fits, the measurement shows at least confi- dently that the crystallites have an ultrafine size, not in the very nanoscale, which is sufficient accuracy within the confines of this study. It is therefore reasonable to infer that the ultrafine B4 C particles obtained by the high-energy ball-milling plus annealing are essentially single crystals. Also, despite the annealing treatment, these B4 C single-crystal particles are still expected to be passivated with a B2 O3 surface layer, which is the typically scenario in non-oxide compounds. Note that the annealing treatment alone cannot provide an oxygen-free powder because the ultrafine B4 C particles will spontaneously passivate in contact with air. Its key function is thus only to remove the oxygen impurities introduced during the high-energy ball-milling in air. This is exactly what is observed in the comparison of XPS spectra in Fig. 4, which confirms the surface oxidation of the B4 C particles during milling and the elimination of oxides with the annealing down to the oxygen level in the as-received condi- tion. The B2 O3 removal was further corroborated by measuring the powder weight change with the annealing, which reflected a mass loss of ∼13.75%. Unfortunately, it is not possible to unambiguously detect the presence of WB2 and W2 B5 by XPS using the B 1s core level due to their severe overlap with the signal from B4 C and to the small relative abundance of these two phases, but the XRD pattern leaves no room for doubt.

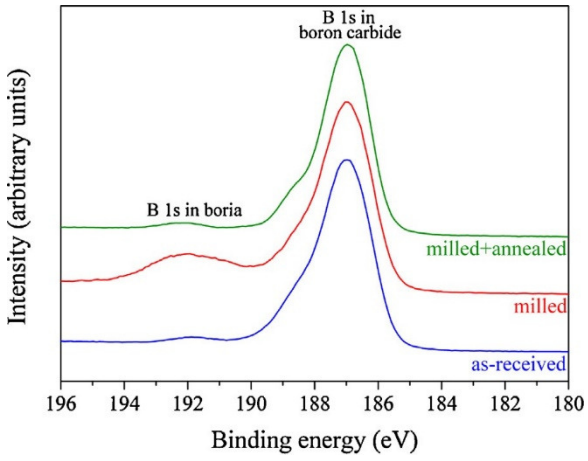

Fig. 4. High-resolution XPS spectra of the B 1s (singlet) core-level for the B4 C powders in the as-received condition, after the high-energy ball-milling, and after the high-energy ball-milling plus annealing. The peak indexing is also included. For the sake of comparison, the XPS spectra have been normalized by imposing the same maximum intensity for the B 1s peak from B4 C, and then shifted along the vertical axis to facilitate their observation.

Fig. 5 shows representative SEM images of the micro- structures obtained under some of the different SPS conditions investigated here. It can be seen in Fig. 5A that the ceramic obtained at 1800 ◦C is nominally dense (>98.5%), although unfortunately this high SPS temperature results in a coarse microstructure with an average B4 C grain size of ∼17 J..m. These large B4 C grains contain microtwins in their interior (originated during SPS because the B4 C particles in the powder used were single-crystals), which is not surprising because B4 C has a low stacking fault energy (i.e., 76 mJ/m2) and is prone to twinning.20 On the contrary, Fig. 5B–D shows that the SPS temperatures from 1700 ◦C downwards are increasingly effective in retain- ing ultrafine-grained microstructures, although the temperature of 1600 ◦C seems to be clearly insufficient to achieve complete densification (i.e., at least 98.5%). Indeed, it became evident during the acquisition of the SEM images that the SPS temperature of 1700 ◦C offered the best compromise in the sought-for objective of densification with retention of ultrafine grains. To confirm this mere visual appreciation and to shed light on the role played by the three SPS parameters varied here (i.e., tar- get temperature, holding time, and heating ramp), the degrees of densification and average grain sizes were measured quantitatively by the Archimedes method and SEM, respectively. The results are listed in Table 1. Firstly, the comparison of the samples labelled as (i) S3–S4, (ii) S5–S6, (iii) S7–S8, and (iv) S10–S11 (each pair of which has the same target temperature and holding time) indicates that the densification is not affected while the grain size increases with increasing heating ramp from 100 to 200 ◦C/min.

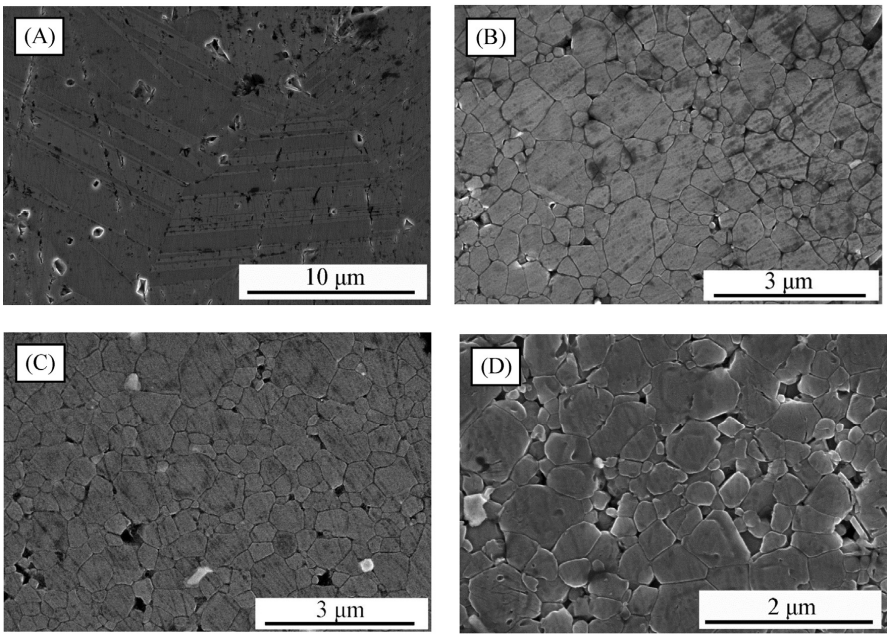

Fig. 5. Representative SEM micrographs of the polished surface of the ceramics obtained from the ultrafine B4 C powder with high-energy ball-milling and annealing by SPS at 75 MPa and: (A) 1800 ◦ C for 3 min with heating ramp of 100 ◦ C/min, (B) 1700 ◦ C for 3 min with heating ramp of 100 ◦ C/min, (C) 1700 ◦ C for 3 min with heating ramp of 200 ◦ C/min, and (D) 1600 ◦ C for 1 min with heating ramp of 200 ◦ C/min. The darker grains are B4 C and the brighter grains are WB2 . Chipping induced during sample preparation is also observed.

This latter is somewhat surprising considering that the higher the heating rates the shorter the time that the powder is exposed to high temperatures. It can, however, be understood by invoking the greater driving force for diffusion induced by the larger thermal gradients as the heating rate increases, and the greater retention of boria at higher temperatures (because the pore structure collapses faster into a closed porosity), both of which effects promote grain growth. The former has already been demonstrated,21,22 and the latter was confirmed here by monitoring the vacuum level during SPS (i.e., it was observed that the release of gas was more gradual and was shifted towards lower temperatures when the heating rate was set at 100 ◦C/min). Additionally, the effect of electric cur- rent as enhancing agent for sintering and grain growth has also been reported, an effect which becomes greater with increasing heating rate.11Secondly, the comparisons (i) S2–S3–S5, (ii) S4–S6, and (iii) S8–S9 (each group of which has the same tar- get temperature and heating ramp) indicate that the densification improves and the grain size increases with increasing holding time, which are the expected trends according to solid-state sintering theory.23 And thirdly, the comparison (i) S1–S3–S7–S10, (ii) S4–S8–S11, and (iii) S6–S9 (each group of which has the same heating rate and holding time) indicates that the densification improves and the grain size increases with increasing target temperature, which again are the expected trends23 because the diffusion coefficients obey an Arrhenius-type law.24 It is also noted that the growth is normal up to 1700 ◦C, but exaggerated at 1800 ◦C. Unfortunately, due to the insufficient set of temperatures and times available, it is not possible to use the grain sizes measured to unambiguously discriminate whether the grain-growth kinetics in the normal growth regime follows the*t* or *Dt* models (i.e., $Dt - D0 = K0 \exp(-Q/RT)t$, where $D0$ is the initial grain size at holding time $t = 0$, Dt the grain size at holding time t, $K0$ is a constant, Q the activation energy for grain growth, R the gas constant, and T the absolute temperature) because they are indistinguishable statistically, an aspect that thus needs further examination in the future.I It can never- theless be anticipated that if the $D2$ kinetics is the appropriate one, then the activation energy for grain growth under SPS (i.e., in the presence of a pulsed electrical current) would presumably lie in the interval 200–300 kJ/mol, whereas in the case of the $D3$ *t* kinetics, the interval would probably be 400–500 kJ/mol.

The comparison of the results in Table 1 with the data reported earlier11 for the ceramics prepared from the as- received powder by SPS at the same uniaxial pressure is also very interesting, and demonstrates the usefulness of the high- energy ball-milling plus annealing to improve the sinterability of B4 C. Thus for example, the as-received powder with particle sizes of 0.5 J..m only reaches 90% density at 1600 ◦C for 5 min, whereas the powder prepared here reaches 94% density at the same temperature with only 3 min of SPS. At 1650 ◦C the two powders already reach the same degree of densification, but the as-received powder requires longer SPS times. Furthermore, the ball-milling plus annealing is also essential to retain ultrafine-grained microstructures since the grain growth factor of the as-received powder is not less than ∼1.4.

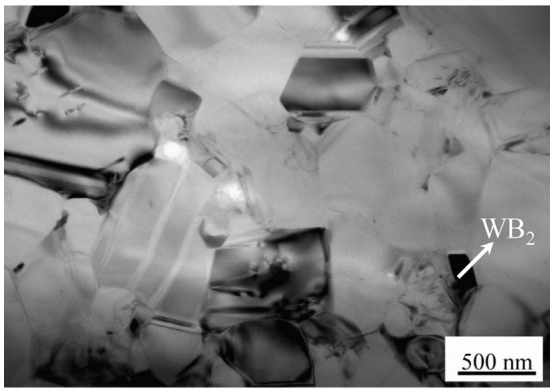

Fig. 6. Representative TEM micrograph of the ceramic resulting from the SPS at 1700 ◦ C for 3 min with heating ramp of 100 ◦ C/min of the ultrafine B4 C powder prepared by high-energy ball-milling plus annealing.

The quantitative results in Table 1 also unambiguously show the SPS at 1700 ◦C for 3 min with 100 ◦C/min to be the most appropriate for successful additive-free processing of ultrafine- grained, dense (i.e., >98.5%) B4 C. Consequently, we shall now characterize microstructurally and mechanically the ceramic thus prepared in greater detail. Fig. 6 is a representative TEM image of its microstructure. It confirms that the ceramic has an equiaxed ultrafine-grain structure, with high dihedral angles at triple joints, and grain boundaries free of glassy phase, as is expected for solid-state sintered materials. The B4 C grain size is the same as that measured by SEM (i.e., ∼370 nm), so that the grain growth factor is about 1.68 (lower factors were actually achieved, but at the expense of porosity). A few of the B4 C grains are seen to be twinned or nanotwinned, but they were the exception, not the rule. Indeed, the average B4 C crystallite size determined from the peak broadening during the Rietveld analysis of the XRD pattern of this sample (Fig. 7) is ∼325 nm; once again, despite the correctness of this measurement may be disputable numerically, it is clear that the crystallite size is beyond the nanoscale which rules out the occurrence of whole- sale nanotwinning. There are also some smaller grains, which were identified as WB2 . These grains retained the small size of the WB2 particles in the powders, or of the WC or W2 B5 particles from which they were formed, because they are iso- lated in the microstructure and therefore there is hardly any W diffusion available for their growth during the rapid SPS. The extensive TEM observations with XEDS analyses never revealed the presence of any other type of grain, indicating that the WC contamination introduced during milling was eventu- ally all transformed to WB2 during the SPS. This is also entirely consistent with the Rietveld analysis, which led to a quantitative phase-composition of 97.1 ± 0.1 wt.% B4 C plus 2.9 ± 0.1 wt.% WB2 (once again with trace amounts of W-rich unidentified phases(s)). Finally, a few nanopores are also observed, but the residual porosity is marginal (i.e., less than 1%).

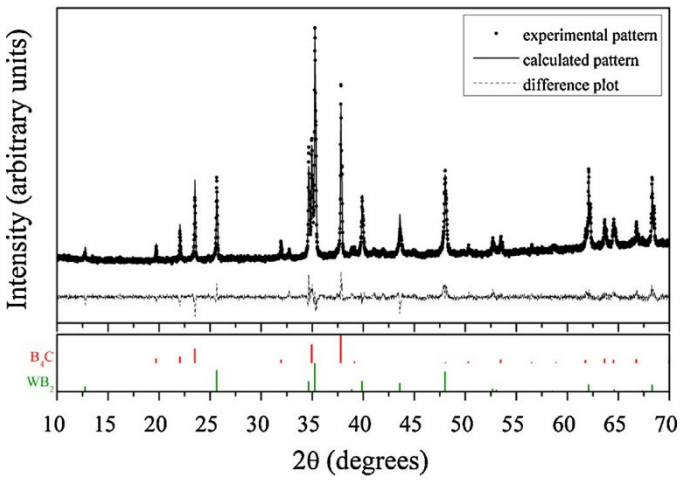

Fig. 7. XRD pattern of the ceramic resulting from the SPS at 1700 ◦ C for 3 min with heating ramp of 100 ◦ C/min of the ultrafine B4 C powder prepared by high- energy ball-milling plus annealing (data point), together with the corresponding Rietveld refinement (solid line). The peak indexing is also included (pdf cards 00-035-0798 and 01-073-1244 for B4 C and WB2 , respectively).

With respect to the mechanical properties, hardness and toughness values of 37.8 GPa and 3.1 MPa m1/2 were measured for this B4 C ceramic. This ultrafine-grained B4 C ceramic is thus slightly harder than its counterpart of 690 nm average grain size fabricated from the as-received powder under identical SPS conditions (i.e., 36.4 GPa),11 which is because the hard- ness scales inversely with the grain size (i.e., the Hall–Petch law [25]). Also, as is observed in Table 1, this is the hardest of all ultrafine-grained B4 C ceramics prepared in the present work. This is due either to its smaller grain size, its greater degree of densification, or the combination of both factors. Furthermore, this ultrafine-grained ceramic is almost equally as tough as its submicrometric-grained counterpart11 because in both cases the fracture mode is essentially transgranular with little intergranu- lar crack propagation, as has been reported elsewhere for the latter11 and verified here for the former by SEM observations of the crack propagation pattern (Fig. 8A; cf. the relatively straight propagation of the crack with barely any deflection, and the rel- ative lack of crack bridging) and of the fracture surface of the broken sample (Fig. 8B; cf. the cleavage steps and features much larger than the 370 nm average grain size; the WB2 grains seem to fracture intergranularly, but this is insufficient to effectively impact on the fracture behaviour). Higher toughness values were measured for the ultrafine-grained ceramics prepared at 1650 ◦C, but that is simply an artefact associated with their greater residual porosity.

Having demonstrated the feasibility of the processing of additive-free superhard B4C ceramics with ultrafine-grained, dense, microstructures, the next step will be to optimize this process for the subsequent B4 C nanostructuring (with the anticipation of further

increasing the hardness). This in turn will rely on the ability (i) to obtain high-purity (virtually oxygen-free) B4 C nanopowders with improved sinterability, so that key issues will be the optimization of the high-energy ball-milling condi- tions and of the corresponding thermal/surface treatments of oxide elimination, or alternatively of protection against surface passivation, and (ii) to control the SPS cycle to retain in as far as possible the nanostructure of these unique B4 C nanopowders. This processing challenge and the evaluation of the mechanical properties of these B4 C nanoceramics will, however, be deferred for future work.

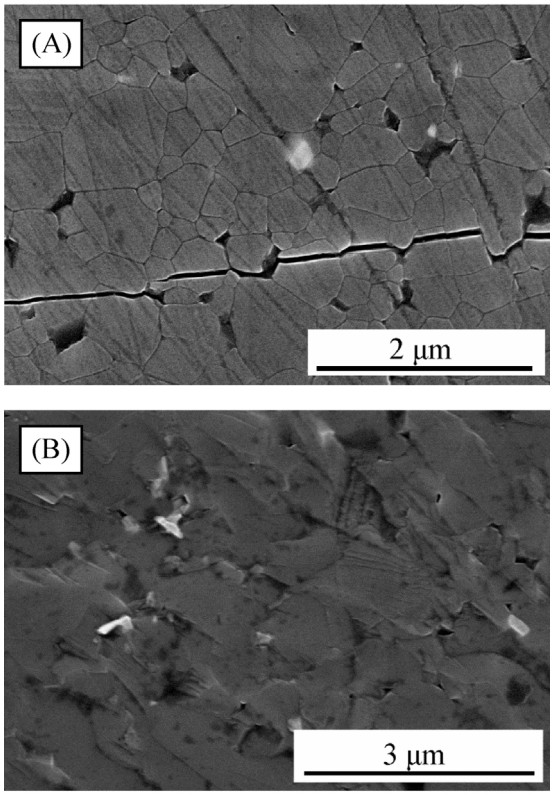

Fig. 8. Representative SEM micrograph of (A) the crack propagation and (B) the fracture surface of the broken ceramic resulting from the SPS at 1700 °C for 3 min with heating ramp of 100 °C/min of the ultrafine B_4C powder prepared by high-energy ball-milling plus annealing. The darker grains are B_4C and the brighter grains are WB_2.

4. Concluding remarks

We have used high-energy ball-milling in air, followed by annealing at moderate temperatures in Ar, to prepare an ultrafine B4 C powder, which was then used to process, by SPS without additives, superhard B4 C ceramics with ultrafine-grained and dense microstructures. Without the annealing post-treatment, the ball-milled powder had

poor sinterability, resulting in porous ceramics at the moderate temperatures required to retain ultrafine grains. The parametric SPS study showed that both the degree of densification and the grain size increase with increasing temperature and holding time, as is also the case for the grain size with increasing heating ramp. It also showed that 1700 ◦C for 3 min with a heating ramp of 100 ◦C/min is the appropriate condition for the complete densification of that B4 C powder with retention of ultrafine grains. Well above 1700 ◦C there is notable grain growth, whereas well below the densification is incomplete. The thus-obtained B4 C ceramic exhibited a hardness value which was as high as ∼38 GPa due to its ultrafine grain size, and without any relevant loss of toughness (∼3 MPa m1/2) relative to its counterparts with coarser micro- structures because, in both cases, the predominant fracture mode is transgranular fracture. Finally, this work proposes the way for the future nanostructuring of the B4 C ceramics, although this will require further optimization of the combination of high-energy ball-milling, powder surface treatment, and SPS.

Acknowledgements

The researchers at the University of Seville acknowledge the financial support by the Spanish Ministerio de Economía y Competitividad under the Grant N◦ MAT2012-38205-C02-01. The work at the University of Extremadura was supported by the Ministerio de Ciencia y Tecnología (Government of Spain) under Grant N◦ MAT 2010-16848.

References

1. Shaffer PTB. Engineering properties of carbides. In: Schneider SJ, editor.

ASTM engineered materials handbook. Vol. 4 – Ceramics and Glasses. Ohio: Materials Park; 1991. p. 804–11.

2. Thevenot F. Boron carbide – a comprehensive review. *J Eur Ceram Soc*

1990;**6**(4):205–25.

3. Domnich V, Reynaud S, Haber RA, Chhowalla M. Boron carbide: structure, properties, and stability under stress. *J Am Ceram Soc* 2011;**94**(11):3605–28.

4. Lee WE, Gilbert M, Murphy ST, Grimes RW. Opportunities for advanced ceramics and composites in the nuclear sector. *J Am Ceram Soc*

2013;**96**(7):2005–30.

5. Suri AK, Subramanian C, Sonber JK, Murthy TSR-Ch. Synthesis and con- solidation of boron carbide: a review. *Int Mater Rev* 2010;**55**(1):4–40.

6. Xu C, Cai Y, Flodström K, Li Z, Esmaeilzadeh S, Zhang GJ. Spark plasma sintering of B4 C ceramics: the effects of milling medium and TiB2 addition. *Int J Refract Met Hard Mater* 2012;**30**(1):139–44.

7. Ghosh D, Subhash G, Sudarshan TS, Radhakrishnan R, Gao XL. Dynamic indentation response of fine-grained boron carbide. *J Am Ceram Soc*

2007;**90**(6):1850–7.

8. Hayun S, Paris V, Dariel MP, Frage N, Zaretzky E. Static and dynamic mechanical properties of boron carbide processed by spark plasma sintering. *J Eur Ceram Soc* 2009;**29**(16):3395–400.

9. Kim KH, Chae JH, Park JS, Ahn JP, Shim KB. Sintering behavior and mechanical properties of B4 C ceramics fabricated by spark plasma sintering. *J Ceram Process Res* 2009;**10**(6):716–20.

10. Hayun S, Kalabukhov S, Ezersky V, Dariel MP, Frage N. Microstructural characterization of spark plasma sintered boron carbide ceramics. *Ceram Int* 2010;**36**(2):51–7.

11. Moshtaghioun BM, Cumbrera-Hernández FL, Gómez-García D, de Bernardi-Martín S, Domínguez-Rodríguez A, Monshi A, Abbasi MH. Effect of spark plasma sintering parameters on microstructure and room- temperature hardness and toughness of fine-grained boron carbide (B4 C). *J Eur Ceram Soc* 2013;**33**(2):361–9.

12. Moshtaghioun BM, Ortiz AL, Gómez-García D, Domínguez-Rodríguez A.

Toughening of super-hard ultra-fine grained B4 C densified by spark-plasma sintering via SiC addition. *J Eur Ceram Soc* 2013;**33**(8):1395–401.

13. Zamora V, Ortiz AL, Guiberteau F, Nygren N. Spark-plasma sintering of ZrB2 ultra-high-temperature ceramics at lower temperature via nanoscale crystal refinement. *J Eur Ceram Soc* 2012;**32**(10):2529–36.

14. Schwets KA, Grellner W. The influence of carbon on the microstructure and mechanical properties of sintered boron carbide. *J Less-Common Met*

1981;**82**:37–47.

15. Dole SL, Prochazka S, Doremus RH. Microstructural coarsening during sintering of boron carbide. *J Am Ceram Soc* 1989;**72**(6):958–66.

16. Walker LS, Pinc WR, Corral EL. Powder processing effects on the rapid low-temperature densification of ZrB2 . *J Am Ceram Soc* 2012;**95**(1):194–203.

17. McCusker LB, Von Dreele RB, Cox DE, Louër D, Scardi P. Rietveld refine-

ment guidelines. *J Appl Crystallogr* 1999;**32**(1):36–50.

18. Green DJ. *An introduction to the mechanical properties of ceramics*.

Cambridge, UK: Cambridge University Press; 1998.

19. Anstis GR, Chantiku1 P, Marshall DB, Lawn BR. A critica! evaluation of indentation techniques for measuring fracture toughness: I. Direct crack measurements. *J Am Ceram Soc* 1981;64(9):533-8.

20. Ashbee KHG. Defects in boron carbide before and after neutron irradiation. *Acta Metall* 1971;**19**(10):1079–85.

21. Young RM, McPherson R. Temperature-gradient driven diffusion in rapid rate sintering. *J Am Ceram Soc* 1989;**72**(6):1080–1.

22. Beruto D, Botter R, Searcy AW. Influence of temperature gradients on sintering: experimental tests of a theory. *J Am Ceram Soc* 1989;**72**(2):232–5.

23. German RM. *Sintering theory and practice*. New York, USA: Wiley; 1996.

24. Poirier DR, Geiger GH. *Transport phenomena in materials processing*. Pennsylvania, USA: The Minerals Metals & Materials Society; 1998.

25. Meyers MA, Mishra A, Benson DJ. Mechanical properties